

Theory of the Uhlmann Phase in Quasi-Hermitian Quantum Systems

Xu-Yang Hou,¹ Xin Wang,¹ and Hao Guo^{1,2,*}

¹*School of Physics, Southeast University, Jiulonghu Campus, Nanjing 211189, China*

²*Hefei National Laboratory, University of Science and Technology of China, Hefei 230088, China*

Geometric phases play a fundamental role in understanding quantum topology, yet extending the Uhlmann phase to non-Hermitian systems poses significant challenges due to parameter-dependent inner product structures. In this work, we develop a comprehensive theory of the Uhlmann phase for quasi-Hermitian systems, where the physical Hilbert space metric varies with external parameters. By constructing a generalized purification that respects the quasi-Hermitian inner product, we derive the corresponding parallel transport condition and Uhlmann connection. Our analysis reveals that the dynamic metric induces emergent geometric features absent in the standard Hermitian theory. Applying this formalism to solvable two-level models, we uncover rich finite-temperature topological phase diagrams, including multiple transitions between trivial and nontrivial phases driven by thermal fluctuations. Crucially, the quasi-Hermitian parameters are shown to profoundly influence the stability of topological regimes against temperature, enabling nontrivial phases to persist within finite-temperature windows. Furthermore, by extending established interferometric protocols originally developed for Hermitian systems, the geometric amplitude can be recast as a measurable Loschmidt fidelity between purified states, providing a practical and experimentally accessible pathway to investigate quasi-Hermitian mixed-state geometric phases and their finite-temperature transitions. This work establishes a unified framework for understanding mixed-state geometric phases in non-Hermitian quantum systems and opens a practical avenue for their experimental investigation.

I. INTRODUCTION

The geometric phase, since its modern formulation by Berry, has proven to be a fundamental concept permeating diverse areas of quantum physics, from the dynamics of adiabatic systems to the characterization of topological phases of matter [1, 2]. While the Berry phase provides a robust framework for pure quantum states, realistic physical systems are invariably open, interacting with their environment and existing at finite temperature. This has motivated a long-standing quest to generalize geometric phases to mixed quantum states, described by density matrices. Several approaches have been developed in this direction, including the interferometric geometric phase proposed by Sjöqvist et al. [3], which has been extensively studied [4–6] and observed in various experimental platforms such as nuclear magnetic resonance [7], polarized neutrons [8], and Mach-Zehnder interferometry [9]. Another important mathematical generalization, formulated independently by Uhlmann, provides a fiber bundle description in which a geometric phase is accumulated via the parallel transport of the amplitude of a density matrix [10–13]. This approach, now known as the Uhlmann phase, has gained considerable attention for its deep geometric structure and its relevance to condensed matter and quantum information [14–21]. This phase has proven instrumental in exploring the finite-temperature topology of condensed matter systems [22–30].

Thus far, however, these developments have largely remained within the framework of Hermitian quantum mechanics. Meanwhile, a vast and rapidly growing class of

physical systems is described by non-Hermitian Hamiltonians, which have uncovered many fascinating phenomena including Anderson localization [31], unconventional behavior of quantum emitters [32, 33], and distinctive topological properties [34–36]. Theoretical and experimental investigations of non-Hermitian topology have since flourished, revealing unique phenomena such as non-Hermitian skin effects and novel bulk-boundary correspondences [37–43]. The notion of geometric phase has been extended to non-Hermitian systems [44], and subsequently applied to construct the quantum geometric tensor for such systems [45]. Among non-Hermitian frameworks, pseudo-Hermitian and, more specifically, quasi-Hermitian systems stand out, as they possess real spectra and admit a consistent quantum mechanical interpretation through the construction of a physically admissible positive-definite metric operator η_+ [46–50]. A major branch includes systems with parity-time reversal (\mathcal{PT}) symmetry, which has attracted considerable research attention [47, 51–56] and has been experimentally realized across acoustics, optics, electronics, and quantum systems [57, 58]. The dynamics and geometry of such systems are defined not by the standard Dirac inner product, but by a physical inner product $(\cdot, \cdot)_{\eta_+} = \langle \cdot | \eta_+ | \cdot \rangle$ that generally depends on the system's parameters [59, 60]. This parameter-dependent inner product fundamentally alters the geometric structure of the Hilbert space, raising a critical question: how should the geometric phase of mixed states be understood in such a setting?

In this work, we address this question by developing a comprehensive theory of the Uhlmann phase for quasi-Hermitian quantum systems at finite temperature. Our motivation is twofold. First, the need to describe realistic systems inherently subject to environmental influences

* guohao.ph@seu.edu.cn

and thermal fluctuations naturally calls for a mixed-state geometric framework. Extending this framework to encompass the quasi-Hermitian paradigm is essential for a complete description of open or non-Hermitian systems in thermal equilibrium. Second, the geometric properties of mixed states in quasi-Hermitian systems are expected to differ profoundly from those of their pure-state counterparts. Unlike the Berry phase, which for a quasi-Hermitian system is governed by adiabatic evolution under a single Hamiltonian, the Uhlmann phase involves the parallel transport of a purification and is sensitive to the system's statistical mixture. The interplay between this statistical mixing and the parameter-dependent metric $\eta_+(\lambda)$ is anticipated to give rise to novel geometric features not captured by either the standard Uhlmann theory or the quasi-Hermitian Berry phase alone.

A central observation underlying our construction is that the standard purification $\rho = WW^\dagger$, used ubiquitously in conventional Uhlmann theory, is no longer valid for quasi-Hermitian systems, as it would implicitly force the density matrix to be Hermitian. To overcome this fundamental obstruction, we instead decompose the density matrix using the \ddagger -operation defined by the physical metric $\eta_+(\lambda)$: $\rho = WW^\ddagger$, where W is the amplitude or purification. In this framework, the gauge redundancy is naturally described by the quasi-unitary group $U_{\eta_+}(N)$, whose elements satisfy $U^\ddagger U = \mathbb{I}$. Consequently, the amplitude can be expressed as $W = \sqrt{\rho}U$, with $U \in U_{\eta_+}(N)$ serving as the generalized phase factor that replaces the unitary factor of the Hermitian theory. This construction faithfully reflects the underlying metric structure and provides the proper starting point for generalizing the Uhlmann formalism to the quasi-Hermitian realm. By imposing a parallel transport condition based on minimizing the η_+ -weighted Hilbert-Schmidt distance between neighboring amplitudes, we derive the corresponding Uhlmann connection \mathcal{A}_U^η and the holonomy that defines the quasi-Hermitian Uhlmann phase θ_U^η . We show that this geometric structure is uniquely determined by the parameter dependence of both the density matrix and the metric, thereby capturing the subtle interplay between statistical mixing and the evolving physical inner product.

To illustrate the physical implications of our formalism, we apply it to two exactly solvable two-level models. The first features a parameter-independent metric and serves as a baseline, while the second, a \mathcal{PT} -symmetric model, exhibits a genuinely parameter-dependent metric, allowing us to showcase the novel geometric effects arising from the dynamical inner product. Our analysis reveals that the Uhlmann phase can undergo distinctive finite-temperature topological phase transitions, driven by the interplay of thermal fluctuations and non-Hermitian parameters. Remarkably, the parameter-dependent metric $\eta_+(\lambda)$ does not merely provide a static background; it actively participates in the geometric evolution, inducing an emergent geometric contribution entirely absent in the Hermitian limit. This fundamentally al-

ters the finite-temperature phase diagram, revealing a much richer structure than previously anticipated. Finally, we elucidate the relationship between our quasi-Hermitian construction and the standard Uhlmann theory by examining the effect of a parameter-dependent similarity transformation that maps the quasi-Hermitian system to a Hermitian representation. This analysis reveals that the two frameworks, while describing the same physics, are connected through a nontrivial, metric-induced gauge structure. The dynamic inner product, encoded in $d\eta_+(\lambda)$, gives rise to an additional connection term that fundamentally alters the parallel transport rule for the purified states. This finding highlights that the local geometry of mixed states in quasi-Hermitian systems is far richer than in their Hermitian counterparts and is intimately linked to the broader context of quantum geometric tensors for mixed states.

Our work establishes a unified geometric framework for mixed states in quasi-Hermitian systems, paving the way for exploring finite-temperature topology and geometry in a wide range of non-Hermitian physical settings, from open quantum systems to correlated materials. The remainder of this paper is organized as follows. In Sec. II, we review the quasi-Hermitian framework and establish the parameter-dependent metric structure. In Sec. III, we construct the quasi-Hermitian Uhlmann formalism based on the η_+ -weighted purification scheme and derive the corresponding connection and Uhlmann phase. In Sec. IV, we discuss two solvable two-level examples with parameter-independent and parameter-dependent metrics, respectively, and examine the associated finite-temperature geometric phase transitions. In Sec. V, we discuss an experimentally feasible interferometric protocol for measuring the quasi-Hermitian Uhlmann phase. Finally, Sec. VI presents our conclusions and outlook.

II. MATHEMATICAL DESCRIPTION OF QUASI-HERMITIAN MIXED STATES

A. Definitions and Basic Properties of Quasi-Hermitian Systems

In non-Hermitian quantum systems, a fundamental challenge is to establish a consistent probabilistic interpretation and geometric structure while preserving dynamical consistency. If a Hamiltonian is not Hermitian under the standard Dirac inner product, its time evolution operator is generally non-unitary, thereby breaking probability conservation and the standard geometric structure of the state space. Pseudo-Hermitian quantum mechanics provides a systematic resolution to this problem. Its basic idea is not to abandon the Hermiticity principle of quantum mechanics, but rather to treat the inner product structure itself as part of the theory, reconstructing the physical Hilbert space by an appropriate choice of a physical metric.

Specifically, if there exists a linear, Hermitian, and in-

vertible operator η such that the Hamiltonian satisfies

$$H^\dagger = \eta H \eta^{-1}, \quad (1)$$

then H is called a pseudo-Hermitian operator [59]. This condition indicates that H and its Hermitian conjugate are equivalent under a similarity transformation, imposing strict constraints on its spectral structure. However, in general, η does not guarantee the positivity of the inner product. Therefore, pseudo-Hermiticity alone is insufficient to establish a complete probabilistic framework for quantum mechanics.

When the metric operator is further required to be positive-definite and Hermitian, denoted as η_+ , the system enters the quasi-Hermitian regime. In this case, a new physical inner product can be defined via η_+ :

$$(\phi, \psi)_{\eta_+} := \langle \phi | \eta_+ | \psi \rangle, \quad (2)$$

thereby introducing a new Hilbert space structure $(\mathcal{H}, (\cdot, \cdot)_{\eta_+})$ on the same vector space. Under this physical inner product, quasi-Hermitian systems exhibit real energy spectra and possess a complete and consistent probabilistic interpretation for their dynamics [60].

In the quasi-Hermitian framework, the concepts of “self-adjointness” and “observables” must be generalized accordingly. Defining the η_+ -adjoint operation

$$A^\ddagger := \eta_+^{-1} A^\dagger \eta_+, \quad (3)$$

physical observables are required to satisfy the η_+ -self-adjoint condition $O^\ddagger = O$. This definition ensures the reality of expectation values for observables and the consistency of the probabilistic interpretation under the physical inner product. Thus, quasi-Hermitian quantum mechanics does not abandon the fundamental principle of Hermiticity; rather, it extends it from the fixed Dirac inner product to the physical inner product determined by the metric operator.

It is worth noting that in many practical problems, the Hamiltonian depends on a set of external parameters λ , and the compatible positive-definite metric operator may also vary with these parameters, i.e., $\eta_+ = \eta_+(\lambda)$. In such cases, although the system can be considered quasi-Hermitian at each fixed parameter point, the inner product structure of the physical Hilbert space itself evolves along the parameter path. The primary goal of this paper is to systematically investigate the new Hilbert space geometry introduced by this variation of the inner product structure and to explore its influence on the geometric phase of mixed states.

B. Spectral Structure and Equilibrium Density Matrix of Quasi-Hermitian Systems

It must be emphasized that the self-adjointness of H established above is with respect to the η_+ -inner product; under the standard Dirac inner product, H generally

remains non-Hermitian. Consequently, even with a real spectrum, its eigenstate structure differs fundamentally from that of Hermitian systems.

Specifically, let the right eigenstates of the quasi-Hermitian Hamiltonian H satisfy

$$H |\Psi_n\rangle = E_n |\Psi_n\rangle. \quad (4)$$

Since the spectrum E_n is real, one can correspondingly introduce the left eigenstates of H^\dagger :

$$H^\dagger |\Phi_n\rangle = E_n |\Phi_n\rangle. \quad (5)$$

Under the Dirac inner product, these two sets of eigenstates generally do not coincide. However, in the non-degenerate case, they can be chosen to satisfy the biorthogonality relations

$$\langle \Phi_m | \Psi_n \rangle = \delta_{mn}, \quad \sum_n |\Psi_n\rangle \langle \Phi_n| = \mathbb{I}. \quad (6)$$

This biorthogonal representation, constituted by left and right eigenstates, is a standard structure in quasi-Hermitian spectral theory and provides a natural framework for achieving a consistent spectral decomposition in the quasi-Hermitian representation.

In quasi-Hermitian systems, there exists a direct connection between the biorthogonal structure and the physical inner product. Since H satisfies the self-adjoint condition $H^\ddagger = H$ under the η_+ -inner product, the left and right eigenstates can be related through the metric operator. Under an appropriate gauge choice, we may take

$$|\Phi_n\rangle = \eta_+ |\Psi_n\rangle, \quad (7)$$

so that the right eigenstates satisfy the orthonormality relation under the physical inner product:

$$(\Psi_m, \Psi_n)_{\eta_+} = \langle \Psi_m | \eta_+ | \Psi_n \rangle = \delta_{mn}. \quad (8)$$

This demonstrates that the biorthogonal representation is not in conflict with the physical Hilbert space; rather, it is a concrete manifestation of the positive-definite inner product structure within the non-Hermitian representation of quasi-Hermitian systems. Under the biorthogonal spectral structure described above, the quasi-Hermitian Hamiltonian can be decomposed as

$$H = \sum_n E_n |\Psi_n\rangle \langle \Phi_n|, \quad (9)$$

a form analogous to the spectral decomposition in Hermitian systems, but with orthogonality in the state space characterized by the biorthogonal relations.

We now turn to the statistical description of mixed states within the quasi-Hermitian framework. In direct analogy with the Hermitian case, the equilibrium density matrix is defined as

$$\rho \equiv \frac{e^{-\beta H}}{Z}, \quad Z = \sum_n e^{-\beta E_n} = \text{Tr}_{\eta_+}(e^{-\beta H}), \quad (10)$$

where $\beta = 1/T$ is the inverse temperature. Here the physical trace Tr_{η_+} is defined by

$$\begin{aligned} \text{Tr}_{\eta_+}(A) &:= \text{Tr}(\eta_+ A) \\ &= \sum_n \langle \Psi_n | \eta_+ A | \Psi_n \rangle = \sum_n \langle \Phi_n | A | \Psi_n \rangle, \end{aligned} \quad (11)$$

which, in the spectral representation, coincides with the biorthogonal trace [59]. Using the quasi-Hermitian condition $H^\ddagger = H$, one finds that the density matrix satisfies $\rho^\ddagger = \rho$, confirming that ρ is self-adjoint under the physical inner product and therefore represents a legitimate physical mixed state.

Furthermore, as an analytic function of H , the density matrix admits a spectral decomposition in the biorthogonal basis analogous to Eq. (9):

$$\rho = \sum_n p_n |\Psi_n\rangle\langle\Phi_n|, \quad p_n = \frac{e^{-\beta E_n}}{Z}, \quad (12)$$

where the weights p_n are identical to the Gibbs distribution in Hermitian systems. The eigenvalues are non-negative and sum to unity, ensuring the standard probabilistic interpretation.

Thus, we have established the basic statistical description of mixed states within the quasi-Hermitian framework. Although the Hamiltonian is non-Hermitian in the Dirac representation, the introduction of a positive-definite metric operator restores self-adjointness and probabilistic consistency in the physical Hilbert space, yielding a spectral representation built upon the biorthogonal basis. This structure provides the necessary foundation for the subsequent introduction of the geometric phase of mixed states.

III. THEORETICAL FRAMEWORK OF UHLMANN PHASE IN QUASI-HERMITIAN SYSTEMS

When a quasi-Hermitian system depends on a set of tunable external parameters λ , both the Hamiltonian and the metric operator typically become functions of these parameters, i.e., $H(\lambda)$ and $\eta_+(\lambda)$. Together, they determine the physical inner product structure along the parameter path. Unlike in Hermitian systems, in the quasi-Hermitian case the inner product of the physical Hilbert space itself evolves with the parameters. This parameter-dependent inner product fundamentally alters the geometric properties of the state space, raising a natural question: how should one define and characterize the geometric phase acquired by a mixed state when such a system undergoes a cyclic evolution in parameter space?

To address this question, we develop a geometric framework for mixed states in quasi-Hermitian systems by generalizing Uhlmann's construction of geometric phases for density matrices. The central idea is to represent each mixed state ρ by an amplitude operator W satisfying $\rho = WW^\ddagger$, where the \ddagger -operation is defined with

respect to the parameter-dependent metric $\eta_+(\lambda)$. This representation lifts the evolution of mixed states in the parameter space to a path in a higher-dimensional amplitude space. The price we pay for this lift is the introduction of a gauge redundancy: different amplitudes related by $W \rightarrow WU$ with $U^\ddagger U = \mathbb{I}$ represent the same physical mixed state. This gauge freedom, governed by the quasi-unitary group $U_{\eta_+}(N)$, provides the language needed to separate geometric effects from dynamical ones. By imposing a parallel transport condition that selects a “natural” lift of the path in a way that minimizes the distance between neighboring amplitudes, we obtain a connection whose holonomy along a closed loop defines the geometric phase—the quasi-Hermitian Uhlmann phase. The key distinction from the Hermitian case is that the gauge group itself depends on the parameters through the metric $\eta_+(\lambda)$, introducing new geometric features that we will explore in detail.

A. Purification and Gauge Structure of Quasi-Hermitian Mixed States

To make the above construction explicit, we introduce the amplitude operator W , also called a purification, satisfying

$$\rho = WW^\ddagger, \quad (13)$$

where \ddagger denotes the η_+ -adjoint operation defined with respect to the physical inner product. This representation lifts the mixed state density matrix ρ to a point W in the purification space.

The purification representation (13) is not unique. If W is a purification of ρ , then for any invertible operator U satisfying

$$U^\ddagger U = \mathbb{I}, \quad (14)$$

the operator WU describes the same mixed state, i.e., corresponds to the same density matrix ρ . Thus, we have the equivalence relation

$$W \sim WU. \quad (15)$$

The gauge group preserving the physical inner product is the quasi-unitary group $U_{\eta_+}(N)$, which replaces the unitary group $U(N)$ of the Hermitian case. For a full-rank density matrix, any purification can be written as

$$W = \sqrt{\rho} U, \quad (16)$$

where $\sqrt{\rho}$ is the positive square root of ρ in the quasi-Hermitian Hilbert space. Under biorthogonal spectral decomposition, $\sqrt{\rho} = \sum_n \sqrt{p_n} |\Psi_n\rangle\langle\Phi_n|$, encoding the spectral structure and statistical weights. The factor $U \in U_{\eta_+}(N)$ characterizes the gauge degrees of freedom, playing a role analogous to the phase factor in pure-state geometry.

To complete the geometric description, we note that the purifications in the quasi-Hermitian framework naturally form a Hilbert space $\mathcal{H}_W^{\eta_+}$. A suitable inner product on this space, the quasi-Hermitian Hilbert–Schmidt inner product, can be defined in direct analogy with the standard Hermitian case [61] as

$$(W_1, W_2)_{\text{HS}}^{\eta_+} := \text{Tr}_{\eta_+} \left(W_1^\dagger W_2 \right) = \text{Tr} \left(\eta_+ W_1^\dagger W_2 \right). \quad (17)$$

One can verify that this defines a Hermitian scalar product fully compatible with the underlying quasi-Hermitian inner-product structure.

Following the standard Uhlmann theory, we organize the purification space into a principal bundle: the total space S_N consists of all purifications satisfying the normalization condition; the base space is the manifold of full-rank density matrices D_N^N . The natural projection is

$$\pi : S_N \rightarrow D_N^N, \quad \pi(W) := WW^\dagger = \rho. \quad (18)$$

At any point ρ , the fiber consists of all equivalent purifications,

$$\pi^{-1}(\rho) = \{ W = \sqrt{\rho} U \mid U \in U_{\eta_+}(N) \}. \quad (19)$$

At this point, it is important to clarify the mathematical nature of the structure group in this construction. While the fiber at a point ρ is given by $W = \sqrt{\rho} U$ with U satisfying $U^\dagger U = \mathbb{I}$, the operator \dagger depends explicitly on the metric $\eta_+(\lambda)$. Consequently, the set of such U forms the quasi-unitary group $U_{\eta_+(\lambda)}(N)$, which itself varies with the parameter λ . Strictly speaking, a principal bundle is defined with a fixed structure group G that does not depend on the base point. Therefore, our construction is not a principal bundle in the conventional sense. Instead, it can be more rigorously understood as a reduction of structure group of a larger, fixed principal bundle, specifically, a $GL(N, \mathbb{C})$ -bundle, where the reduction to the subgroup $U_{\eta_+(\lambda)}(N)$ is parameter-dependent. The variation of $\eta_+(\lambda)$ along the parameter space means that we are effectively moving through different reductions of the same ambient $GL(N, \mathbb{C})$ -bundle. For the purpose of constructing the Uhlmann phase via parallel transport along a given path $\rho(\lambda)$, this subtlety does not affect our local computations. At each fixed λ , $U_{\eta_+(\lambda)}(N)$ serves as the effective symmetry group governing the fiber directions. The parallel transport condition and the resulting connection to be introduced below are defined with respect to this λ -dependent group, which is sufficient for defining the holonomy and the geometric phase along a closed loop in the extended parameter space.

This constitutes the geometric skeleton of the quasi-Hermitian Uhlmann bundle: the base space is the manifold of density matrices, the total space is the amplitude space, the fibers correspond to the quasi-unitary gauge degrees of freedom, and the structure group is generalized from $U(N)$ to $U_{\eta_+}(N)$. On this basis, introducing an

appropriate parallel transport condition will allow us to further define the quasi-Hermitian Uhlmann connection and the corresponding holonomy.

B. Uhlmann Phase in Quasi-Hermitian Systems

To extract the geometric phase, we must select a horizontal lift of the path $\rho(\lambda)$ to the purification space. This is achieved by imposing a parallel transport condition that minimizes the Hilbert-Schmidt distance between neighboring purifications [62].

To this end, we introduce the Hilbert-Schmidt distance in the quasi-Hermitian purification space. For two purification operators W_1 and W_2 , we define

$$D_{\text{HS}}^2(W_1, W_2) := \text{Tr}_{\eta_+} \left[(W_1 - W_2)^\dagger (W_1 - W_2) \right]. \quad (20)$$

Since purifications possess gauge redundancy, their lifted paths can be adjusted by $U(\lambda)$. This condition selects, within the gauge degrees of freedom, the lift that minimizes this distance between neighboring purifications. Its continuous limit equivalently yields

$$W^\dagger(\lambda) \dot{W}(\lambda) = \dot{W}^\dagger(\lambda) W(\lambda), \quad (\dot{}) \equiv \frac{d}{d\lambda}. \quad (21)$$

A detailed derivation can be found in Appendix A. This condition is a natural generalization of the standard Uhlmann parallel condition to the η_+ -inner product structure. From a geometric perspective, Eq. (21) selects a horizontal curve in the purification space, thereby distinguishing horizontal variations from gauge (vertical) variations along the fiber directions.

Along a parallel transport path, we define the quasi-Hermitian Uhlmann connection as

$$\mathcal{A}_U^{\eta_+}(\lambda) := -dU(\lambda)U^\dagger(\lambda). \quad (22)$$

From the quasi-unitary condition, we obtain $(\mathcal{A}_U^{\eta_+})^\dagger = -\mathcal{A}_U^{\eta_+}$, so $\mathcal{A}_U^{\eta_+}$ takes values in the Lie algebra of the quasi-unitary group $U_{\eta_+}(N)$, fully compatible with the quasi-Hermitian inner product structure. Equivalently, the above expression can be rewritten as the covariant parallel evolution equation for the phase factor:

$$dU + \mathcal{A}_U^{\eta_+} U = 0. \quad (23)$$

Integrating this equation along a loop $\mathcal{C} := \{\rho(\lambda) \mid 0 \leq \lambda \leq \tau, \rho(0) = \rho(\tau)\}$ with path ordering yields

$$U(\tau) = \mathcal{P} \exp \left(- \int_0^\tau \mathcal{A}_U^{\eta_+}(\lambda) \right) U(0), \quad (24)$$

where \mathcal{P} denotes the path-ordering operator. This expression gives the Uhlmann holonomy obtained along a closed parameter path. Geometrically, $\mathcal{A}_U^{\eta_+}(\lambda)$ is the pullback of a connection one-form on the total space to the base space curve $\rho(\lambda)$. The resulting holonomy is

gauge invariant and reflects only the intrinsic geometry of the mixed state path.

The above definition of the quasi-Hermitian Uhlmann connection is not an additional assumption but is uniquely determined by the parallel transport condition. Substituting the gauge decomposition form of the purification into the parallel evolution condition (21) and utilizing the basic properties of the quasi-Hermitian adjoint operation, we obtain a deterministic equation satisfied by the connection $\mathcal{A}_U^{\eta+}$. The result can be organized as

$$\rho \mathcal{A}_U^{\eta+} + \mathcal{A}_U^{\eta+} \rho = -[d\sqrt{\rho}, \sqrt{\rho}]. \quad (25)$$

This equation demonstrates that the quasi-Hermitian Uhlmann connection is completely determined by the variation of the base space path $\rho(\lambda)$ and is independent of specific gauge choices. A detailed derivation is provided in Appendix B.

Substituting the spectral decomposition of the density matrix, Eq. (12), and working in the biorthogonal eigenbasis, the above equation can be solved element-wise, yielding the explicit expression for the quasi-Hermitian Uhlmann connection:

$$\mathcal{A}_U^{\eta+} = - \sum_{i,j} |\Psi_i\rangle \frac{\langle \Phi_i | [d\sqrt{\rho}, \sqrt{\rho}] | \Psi_j \rangle}{p_i + p_j} \langle \Phi_j |. \quad (26)$$

From this connection, we obtain the Hilbert-Schmidt inner product between the initial and final purifications,

$$\mathcal{G} := (W(0), W(\tau))_{\text{HS}}^{\eta+} = \text{Tr}_{\eta+}(\rho(0) U(\tau)), \quad (27)$$

which directly yields the quasi-Hermitian Uhlmann phase

$$\theta_U^{\eta+} = \arg \mathcal{G} = \arg \text{Tr}_{\eta+}[\rho(0) U(\tau)]. \quad (28)$$

When η_+ reduces to the identity, the above results reduce to the Uhlmann phase in Hermitian systems.

To analyze the zero structure of \mathcal{G} and its possible nonanalytic behavior, we introduce, by analogy with the thermodynamic free-energy density, the geometrical generating function [63]

$$g = - \lim_{L \rightarrow \infty} \frac{1}{L} \ln |\mathcal{G}|^2, \quad (29)$$

where L denotes the system size. Nonanalyticities of g occur precisely when \mathcal{G} approaches zero.

IV. TWO-LEVEL MODELS: PARAMETER-INDEPENDENT AND PARAMETER-DEPENDENT METRICS

We now illustrate the general formalism developed above with two analytically solvable two-level models. These examples are chosen to highlight the contrasting roles of the metric: in the first model, the metric is parameter-independent, whereas in the second it varies with external parameters. As we shall see, this distinction has profound consequences for the mixed-state geometric phase.

A. A Simple Two-Level Model with Parameter-Independent Metric

1. Model Definition

We consider a two-level quasi-Hermitian Hamiltonian parameterized by an angle θ and a real deformation parameter $t > 0$:

$$H(\theta) = \begin{pmatrix} \cos \theta & t \sin \theta \\ \frac{\sin \theta}{t} & -\cos \theta \end{pmatrix}. \quad (30)$$

The eigenvalues of H are given by $E_{\pm} = \pm 1$, independent of θ , indicating that the Hamiltonian describes an isospectral family. The corresponding right eigenstates are

$$|\psi_+\rangle = \begin{pmatrix} \cos \frac{\theta}{2} \\ \frac{\sin \frac{\theta}{2}}{t} \end{pmatrix}, \quad |\psi_-\rangle = \begin{pmatrix} \sin \frac{\theta}{2} \\ -\frac{\cos \frac{\theta}{2}}{t} \end{pmatrix}, \quad (31)$$

and the left eigenstates take the form

$$\langle \phi_+ | = \left(\cos \frac{\theta}{2} \quad t \sin \frac{\theta}{2} \right), \quad \langle \phi_- | = \left(\sin \frac{\theta}{2} \quad -t \cos \frac{\theta}{2} \right). \quad (32)$$

These eigenstates satisfy the biorthogonality condition $\langle \phi_m | \psi_n \rangle = \delta_{mn}$. To ensure quasi-Hermiticity, we introduce the positive-definite metric operator

$$\eta_+ = \begin{pmatrix} 1 & 0 \\ 0 & t^2 \end{pmatrix}, \quad (33)$$

which satisfies $H^\dagger = \eta_+ H \eta_+^{-1}$. The physical inner product is thus defined by $(\cdot, \cdot)_{\eta_+} = \langle \cdot | \eta_+ | \cdot \rangle$.

2. Uhlmann Connection and Phase

We now examine the finite-temperature Uhlmann phase associated with this model. The system is assumed to be in thermal equilibrium at inverse temperature $\beta = 1/T$, with the Gibbs state $\rho(\theta) = e^{-\beta H(\theta)}/Z$. At the initial parameter value $\theta = 0$, the Hamiltonian is diagonal, and the density matrix simplifies to

$$\rho(0) = \frac{1}{e^\beta + e^{-\beta}} \begin{pmatrix} e^{-\beta} & 0 \\ 0 & e^\beta \end{pmatrix}, \quad (34)$$

where we adopt the convention that the eigenvalue $+1$ corresponds to the higher energy state.

Following the quasi-Hermitian Uhlmann formalism developed in Sec. III, we compute the Uhlmann connection $\mathcal{A}_U^{\eta+}$ along a path in θ . For the present model, a straightforward calculation using the general expression (26) yields

$$\mathcal{A}_U^{\eta+} = x \begin{pmatrix} 0 & -\frac{t}{2} \\ \frac{1}{2t} & 0 \end{pmatrix} d\theta, \quad x = \frac{2 - e^\beta - e^{-\beta}}{e^\beta + e^{-\beta}}. \quad (35)$$

Consider a closed path in parameter space that winds Ω times around the circle $\theta \in [0, 2\pi\Omega]$. The corresponding Uhlmann holonomy is obtained by path-ordering the exponential of the integrated connection:

$$U(2\pi\Omega) = \exp\left(-2\pi\Omega x \begin{pmatrix} 0 & -t/2 \\ 1/(2t) & 0 \end{pmatrix}\right) = \begin{pmatrix} \cos(\pi\Omega x) & t \sin(\pi\Omega x) \\ \frac{\sin(\pi\Omega x)}{t} & \cos(\pi\Omega x) \end{pmatrix}. \quad (36)$$

Using $x = -(1 - 1/\cosh\beta)$, the Uhlmann fidelity and Uhlmann phase are respectively given by

$$\mathcal{G} = \cos\left(\pi\Omega \left(1 - \frac{1}{\cosh\beta}\right)\right), \quad (37)$$

and

$$\theta_U^{\eta+} = \arg\left[\cos\left(\pi\Omega \left(1 - \frac{1}{\cosh\beta}\right)\right)\right]. \quad (38)$$

Since the cosine function is real, $\theta_U^{\eta+}$ is either 0 or π (mod 2π), depending on the sign of \mathcal{G} .

3. Finite-Temperature Topological Phase Transitions

The Uhlmann phase $\theta_U^{\eta+}$ encodes the geometric properties of thermal states, exhibiting abrupt jumps at critical temperatures that signal topological phase transitions. These discontinuities occur when the cosine argument in Eq. (38) satisfies

$$\pi\Omega \left(1 - \frac{1}{\cosh\beta_{n,c}}\right) = \left(n + \frac{1}{2}\right)\pi, \quad n \in \mathbb{Z}. \quad (39)$$

At these critical temperatures $T_{n,c} = 1/\beta_{n,c}$, the fidelity \mathcal{G} vanishes, rendering $\theta_U^{\eta+}$ ill-defined and marking the boundary between topologically trivial ($\theta_U^{\eta+} = 0$) and nontrivial ($\theta_U^{\eta+} = \pi$) regimes.

For a single winding ($\Omega = 1$), the condition reduces to

$$\frac{1}{\cosh\beta_{n,c}} = \frac{1}{2} - n, \quad n \in \mathbb{Z}. \quad (40)$$

Only two solutions are physically relevant: at infinite temperature ($\beta \rightarrow 0$, corresponding to $n = 1$), the system resides in the trivial phase with $\theta_U^{\eta} = 0$, whereas at zero temperature ($\beta \rightarrow \infty$, corresponding to $n = 0$), it enters the nontrivial phase with $\theta_U^{\eta} = \pi$. Consequently, for $\Omega = 1$, the system undergoes exactly one topological transition from the nontrivial to the trivial regime as temperature increases.

More generally, the winding number Ω dictates the number of phase transitions. As illustrated in Figure 1, the $\Omega = 2$ case exhibits a richer structure: starting from the trivial phase at zero temperature, the system enters a nontrivial phase at an intermediate critical temperature

before returning to the trivial phase at a higher temperature. For $\Omega = 3$, three successive transitions occur, with nontrivial phases emerging in alternating temperature windows.

Thus, the high-temperature limit universally yields a topologically trivial phase, whereas nontrivial topology survives only within specific finite-temperature windows. The winding number Ω serves as a control parameter governing the complexity of the phase diagram, determining both the number and the locations of topological transitions across the temperature spectrum.

Accordingly, the above result coincides exactly with that of a Hermitian spin- $\frac{1}{2}$ system evolving along a meridional loop [20]. This agreement follows from the fact that the metric operator η_+ in the present model is independent of the external parameters. Since the inner-product structure remains unchanged along the entire parameter path, quasi-Hermiticity introduces no additional geometric contributions, and the mixed-state geometric phase reduces to its Hermitian counterpart. A more detailed analysis of this equivalence is presented in Appendix C.

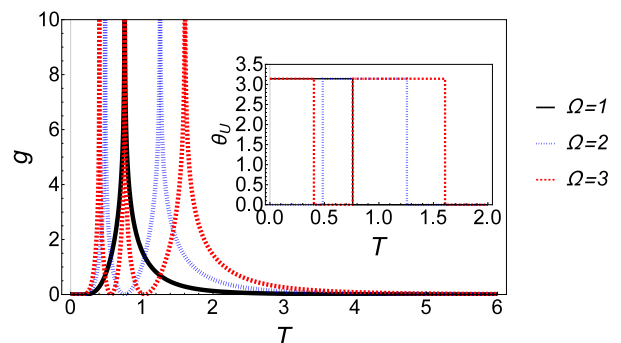


Figure 1. The Uhlmann phase θ_U^{η} (inset) and the geometric factor $g = \cos^{-1}(\mathcal{G})$ as functions of temperature for $\Omega = 1$ (black solid), $\Omega = 2$ (blue dotted), and $\Omega = 3$ (red dashed). The diverging peaks indicate critical temperatures where the phase jumps by π .

B. A \mathcal{PT} -Symmetric Two-Level Model with Parameter-Dependent Metric

While the previous example demonstrates finite-temperature topological phase transitions captured by the Uhlmann phase, the quasi-Hermitian parameter t does not directly influence the value of the Uhlmann phase. We now construct a more intricate example to explicitly showcase the impact of quasi-Hermitian parameters on the geometric structure of quantum states.

1. The \mathcal{PT} -Symmetric Two-Level Model and Its Spectral Structure

We consider a quantum model defined on a two-dimensional Hilbert space. In this setting, any Hermitian 2×2 operator can be expressed as a linear combination of Pauli matrices, naturally corresponding to a direction on the Bloch sphere. As a starting point, we introduce a simple reference Hermitian Hamiltonian

$$H_{2 \times 2} = \hat{e}_r \cdot \vec{\sigma} = \begin{pmatrix} \cos \theta & \sin \theta e^{-i\phi} \\ \sin \theta e^{i\phi} & -\cos \theta \end{pmatrix}, \quad (41)$$

where $\vec{\sigma} = (\sigma_x, \sigma_y, \sigma_z)$ are the standard Pauli matrices, and the unit vector

$$\hat{e}_r = (\sin \theta \cos \phi, \sin \theta \sin \phi, \cos \theta), \quad (42)$$

parametrizes the radial direction on the Bloch sphere. The eigenstates of this Hamiltonian correspond to pure states polarized along \hat{e}_r , with the spectrum and geometric structure controlled entirely by the spherical angles (θ, ϕ) . To avoid confusion with vectors in an arbitrary parameter space \mathbf{X} , we use arrow notation \vec{A} exclusively for vectors in three-dimensional real space.

Building on this, a general \mathcal{PT} -symmetric 2×2 Hamiltonian is characterized by six real parameters $\mathbf{X} = (\varepsilon, a, b, \theta, \phi, \delta)$ and takes the form

$$H_{2 \times 2}(\mathbf{X}) = \varepsilon + (a \hat{e}_r + ib \cos \delta \hat{e}_\theta + ib \sin \delta \hat{e}_\varphi) \cdot \vec{\sigma}, \quad (43)$$

where ε represents a global energy shift, and a and b control the coupling strengths along the radial and tangential directions, respectively. The two orthogonal unit vectors

$$\begin{aligned} \hat{e}_\theta &= (\cos \theta \cos \phi, \cos \theta \sin \phi, -\sin \theta), \\ \hat{e}_\varphi &= (-\sin \phi, \cos \phi, 0), \end{aligned} \quad (44)$$

span the tangent space of the Bloch sphere at the point (θ, ϕ) [64].

This \mathcal{PT} -symmetric Hamiltonian can be understood as a geometric generalization of the Hermitian model $H_{2 \times 2} = \hat{e}_r \cdot \vec{\sigma}$. The component along the radial direction \hat{e}_r remains real, determining the main spectral structure, while the tangential components along \hat{e}_θ and \hat{e}_φ are complexified into purely imaginary terms, introducing non-Hermiticity in a controlled manner. This specific complexification preserves \mathcal{PT} symmetry while maintaining the clear Bloch sphere geometry of the two-dimensional system, providing an ideal minimal model for analyzing mixed-state geometric structures.

The spectrum follows directly from the magnitude of the effective Bloch vector. Using the orthonormal basis $\{\hat{e}_r, \hat{e}_\theta, \hat{e}_\varphi\}$, the two eigenvalues of $H_{2 \times 2}(\mathbf{X})$ are

$$E_\pm = \varepsilon \pm \sqrt{a^2 - b^2}. \quad (45)$$

Thus, the system possesses a non-degenerate real spectrum if and only if $a^2 > b^2$, corresponding to the \mathcal{PT} -unbroken phase where quasi-Hermitian quantum mechanics applies. When $a^2 < b^2$, the spectrum becomes a

complex conjugate pair, and at the critical point $a^2 = b^2$, the eigenvalues coalesce at an exceptional point.

In the following, we focus exclusively on the quasi-Hermitian regime. Within this parameter region, a positive-definite metric operator compatible with the Hamiltonian can be introduced. In the two-dimensional Hilbert space, its explicit form is

$$\eta_+(\mathbf{X}) = \frac{|a|}{\sqrt{a^2 - b^2}} \left(\mathbb{I} + \vec{\beta} \cdot \vec{\sigma} \right), \quad (46)$$

where the vector

$$\vec{\beta} = \frac{b}{a} (\sin \delta \hat{e}_\theta - \cos \delta \hat{e}_\varphi), \quad (47)$$

characterizes the components of the metric operator along the tangent directions of the Bloch sphere. One can verify that η_+ is strictly positive definite, providing the necessary mathematical foundation for constructing the quasi-Hermitian inner product, similarity transformations, and the geometric structure of mixed states.

Under the above quasi-Hermitian conditions, the right eigenstates of $H_{2 \times 2}(\mathbf{X})$ can be chosen as

$$|\psi_\pm\rangle = \frac{1}{\mathcal{N}_\pm} \begin{pmatrix} e^{-i\phi} (a \sin \theta + ib \cos \delta \cos \theta + b \sin \delta) \\ -a \cos \theta + ib \cos \delta \sin \theta \pm \sqrt{a^2 - b^2} \end{pmatrix}, \quad (48)$$

with normalization factors

$$\mathcal{N}_\pm^2 = 2|a|\sqrt{a^2 - b^2} \left[1 + \frac{b}{a} \sin \delta \sin \theta \mp \frac{\sqrt{a^2 - b^2}}{a} \cos \theta \right]. \quad (49)$$

Compared to a generic Hermitian 2×2 Hamiltonian, this \mathcal{PT} -symmetric model introduces two additional independent parameters, offering a minimal platform for exploring the richness of geometric structures in non-Hermitian systems.

2. Uhlmann Connection and Phase on an Equatorial Closed Loop

To simplify analytic calculations, we substitute the spectral decomposition of the density matrix, Eq. (12), into the general expression for the Uhlmann connection, Eq. (26). This yields an alternative form

$$\mathcal{A}_U^{\eta_+} = - \sum_{i \neq j} \frac{(\sqrt{p_i} - \sqrt{p_j})^2}{p_i + p_j} |\Psi_i\rangle \langle \Phi_i| d|\Psi_j\rangle \langle \Phi_j|, \quad (50)$$

where $\{p_i\}$ are the eigenvalues of the density matrix and $\{|\Psi_i\rangle, \langle \Phi_i|\}$ form the quasi-Hermitian biorthogonal eigenbasis. This expression contains only off-diagonal terms, significantly simplifying analytic calculations for two-level systems.

We consider a closed loop on the equator of the Bloch sphere in parameter space, i.e., we fix $\theta = \pi/2$ and let $\phi : 0 \rightarrow 2\pi$, while keeping all other parameters constant. The system is taken to be in the quasi-Hermitian equilibrium state $\rho = e^{-\beta H}/Z$, with $\varepsilon = 0$, $\delta = 0$, and a, b as general real parameters. In the quasi-Hermitian regime $a^2 > b^2$, the energy gap is $\Delta = 2\sqrt{a^2 - b^2}$, and the density matrix eigenvalues are $p_{\pm} = \frac{1}{2} \left(1 \pm \tanh\left(\frac{\beta\Delta}{2}\right) \right)$.

Substituting these results into Eq. (50) and introducing $\kappa = (\sqrt{p_+} - \sqrt{p_-})^2 = 1 - \operatorname{sech}\left(\frac{\beta\Delta}{2}\right)$, the quasi-Hermitian Uhlmann connection along the equatorial path becomes

$$\mathcal{A}_U^{\eta+} = \kappa \left[\frac{2a^2}{\Delta^2} i\sigma_z - \frac{2ab}{\Delta^2} e^{-i\phi\sigma_z/2} \sigma_x e^{i\phi\sigma_z/2} \right] d\phi. \quad (51)$$

The Uhlmann holonomy after one full loop around the equator can be computed explicitly [27, 65]:

$$U(2\pi\Omega) = (-1)^\Omega e^{2\pi\Omega \left[i \left(\frac{2a^2\kappa}{\Delta^2} + \frac{1}{2} \right) \sigma_z - \frac{2ab\kappa}{\Delta^2} \sigma_x \right]}, \quad (52)$$

where Ω denotes the winding number around the equatorial loop. A detailed derivation is provided in Appendix D. Substituting into the expression for the Uhlmann phase, Eq. (28), we obtain

$$\theta_U^{\eta+} = \arg \left[(-1)^\Omega \left(\cos \Theta - \frac{b}{\Delta} \tanh\left(\frac{\Delta\beta}{2}\right) \frac{\sin \Theta}{\gamma} \right) \right], \quad (53)$$

with $\Theta = 2\pi\Omega\gamma$ and $\gamma = \sqrt{\left(\frac{2a^2\kappa}{\Delta^2} + \frac{1}{2}\right)^2 - \left(\frac{2ab\kappa}{\Delta^2}\right)^2}$.

When the non-Hermitian parameter $b = 0$, this result reduces to the Hermitian case [20]. Since the Uhlmann fidelity $\mathcal{G}(\beta)$ is real for this model, the Uhlmann phase along the equatorial loop is completely determined by its sign. When $\mathcal{G}(\beta)$ crosses zero as temperature varies, the Uhlmann phase undergoes a π jump, signaling a geometric phase transition.

In the infinite-temperature limit $\beta \rightarrow 0$, we have $\tanh\left(\frac{\Delta\beta}{2}\right) \rightarrow 0$ and $\kappa \rightarrow 0$, leading to $\gamma \rightarrow \frac{1}{2}$ and $\Theta \rightarrow \pi\Omega$. Since Ω is an integer, the Uhlmann phase satisfies $\theta_U^{\eta+} \rightarrow 0 \pmod{2\pi}$. This indicates that thermal fluctuations wash out the geometric structure at high temperatures, leaving the system in a trivial phase. As temperature decreases, $\mathcal{G}(\beta)$ gradually deviates from its high-temperature limit and crosses zero at certain critical temperatures, inducing π jumps in the Uhlmann phase. These transitions reflect the non-analytic response of the mixed-state geometric phase to temperature and signify finite-temperature geometric phase transitions. Thus, temperature serves as an external parameter controlling the geometric phase structure, driving the system from a trivial high-temperature phase to geometrically non-trivial phases at finite temperatures.

In the zero-temperature limit $\beta \rightarrow \infty$, we obtain $\kappa \rightarrow 1$, $\gamma(\beta) \rightarrow \gamma_0$, and $\tanh\left(\frac{\Delta\beta}{2}\right) \rightarrow 1$. The Uhlmann fidelity can then be written in the form of a phase-shifted cosine:

$$\mathcal{G}(\infty) = (-1)^\Omega \sqrt{1 + A^2} \cos(\Theta_0 + \delta), \quad (54)$$

where

$$\Theta_0 = 2\pi\Omega\gamma_0, \quad A = \frac{b}{\Delta\gamma_0}, \quad \delta = \arctan A. \quad (55)$$

This result shows that in the pure-state limit, the quasi-Hermitian metric effectively introduces a fixed phase shift δ and an effective weight factor γ_0 into the geometric phase. In the Hermitian case, the zero-temperature geometric phase is determined solely by the parity of the winding number Ω , with the criterion simplifying to $\cos(\pi\Omega)$ [20, 27]. In contrast, the quasi-Hermitian system exhibits a much richer oscillatory structure at zero temperature. Figure 2 shows the Uhlmann fidelity $\mathcal{G}(\infty)$ as a function of the winding number Ω for parameters $a = 5$, $b = 4$. The metric effects significantly alter the correspondence between the geometric phase and Ω , leading to geometric features distinctly different from the Hermitian case.

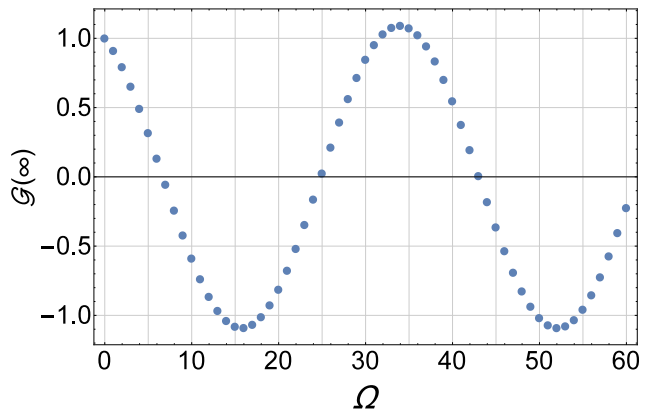


Figure 2. Zero-temperature Uhlmann fidelity $\mathcal{G}(\infty)$ for the quasi-Hermitian two-level model evolving along an equatorial closed loop, plotted as a function of the winding number Ω . Parameters: $\varepsilon = 0$, $a = 5$, $b = 4$, $\delta = 0$.

We now turn to the finite-temperature case. Here, the Uhlmann phase is no longer determined solely by the winding number Ω , but is jointly controlled by temperature T and the non-Hermitian parameter b . As temperature varies, the continuous evolution of the weight factor $\kappa(\beta)$ and the effective parameter $\gamma(\beta)$ reshapes the zero-crossing structure of the Uhlmann fidelity, leading to piecewise jumps and oscillatory behavior in the Uhlmann phase. Figure 3 displays the Uhlmann phase $\theta_U^{\eta+}$ for the quasi-Hermitian two-level model along an equatorial closed loop as a function of temperature T and the quasi-Hermitian parameter b , with the left and right panels corresponding to winding numbers $\Omega = 1$ and $\Omega = 2$, respectively. Yellow regions indicate $\theta_U^{\eta+} = 0$ (topologically trivial phase), while dark blue regions indicate $\theta_U^{\eta+} = \pi$ (topologically nontrivial phase). At infinite temperature, the Uhlmann phase tends to zero, confirming that thermal fluctuations erase the geometric structure. As the non-Hermitian effect strengthens, more geometric phase transitions controlled by the zeros

of the Uhlmann fidelity appear within finite temperature intervals, and the topologically nontrivial regions expand accordingly.

To further reveal the influence of temperature on the geometric phase structure in non-Hermitian systems, Fig. 4 shows the Uhlmann phase as a function of temperature for fixed parameters $a = 5$ and $b = 4$, providing a clearer view of the transition behavior. Compared to the Hermitian spin- $\frac{1}{2}$ case, where only Ω geometric phase transitions occur [20, 27], the quasi-Hermitian case exhibits a more complex temperature response due to off-diagonal contributions introduced by the metric, resulting in additional transition points and a richer phase structure.

Thus, quasi-Hermiticity significantly alters the temperature dependence of the geometric phase. It not only redistributes the locations of geometric phase transitions but also, as the non-Hermitian strength increases, substantially broadens the temperature windows over which non-trivial geometric phases survive. This demonstrates that the geometric structure of quasi-Hermitian mixed states differs fundamentally from the Hermitian case. The special Hilbert space structure modifies how the geometric phase responds to thermal fluctuations and external parameter variations, offering a new avenue for controlling geometric phases in non-Hermitian quantum systems at finite temperatures.

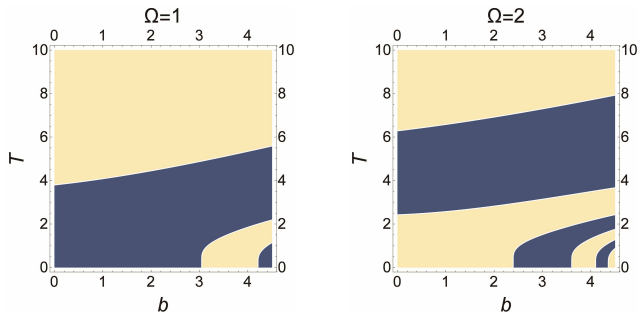


Figure 3. Uhlmann phase $\theta_U^{\eta+}$ for the quasi-Hermitian two-level model along an equatorial closed loop as a function of temperature T and the quasi-Hermitian parameter b . Left and right panels correspond to winding numbers $\Omega = 1$ and $\Omega = 2$, respectively. Yellow: $\theta_U^{\eta+} = 0$ (topologically trivial). Dark blue: $\theta_U^{\eta+} = \pi$ (topologically nontrivial). Parameters: $\varepsilon = 0$, $a = 5$, $\delta = 0$.

V. EXPERIMENTAL REALIZATION

The quasi-Hermitian Uhlmann phase developed in this work is, in principle, experimentally accessible. By embedding the purification formalism into an enlarged Hilbert space, the associated geometric information can be extracted through measurements of the overlap between purified states. Crucially, the quasi-Hermitian Hilbert-Schmidt inner product that characterizes the ge-

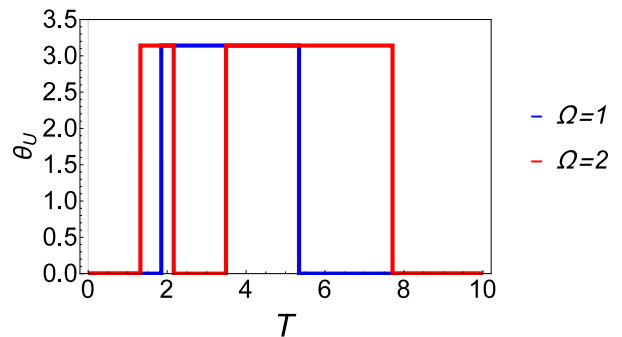


Figure 4. Uhlmann phase $\theta_U^{\eta+}$ for the quasi-Hermitian two-level model along an equatorial closed loop as a function of temperature T . Blue and red solid lines correspond to winding numbers $\Omega = 1$ and 2 , respectively. Parameters: $\varepsilon = 0$, $a = 5$, $b = 4$, $\delta = 0$.

ometric amplitude can be reformulated, within an extended unitary dynamical framework, as a Loschmidt amplitude between two pure states, thereby providing a clear operational route for experimental detection.

Starting from the quasi-Hermitian density matrix $\rho(\lambda)$ introduced in Eq. (12), whose spectral decomposition is given in the biorthogonal basis $\{|\psi_n\rangle, \langle\phi_n|\}$, the corresponding amplitude operator $W = \sqrt{\rho}\mathcal{U}$ can be written in spectral form as

$$W = \sum_n \sqrt{p_n} |\psi_n\rangle \langle\phi_n| \mathcal{U}. \quad (56)$$

To obtain an experimentally accessible formulation, we recast the amplitude operator in its vectorized form, mapping it onto a purified state in an enlarged Hilbert space $\mathcal{H}_S \otimes \mathcal{H}_A$ [62, 63],

$$|W\rangle = \sum_n \sqrt{p_n} |\psi_n\rangle_S \otimes \mathcal{U}^T |\phi_n\rangle_A. \quad (57)$$

This construction establishes an isomorphism between the amplitude space and the tensor-product Hilbert space of the system and an ancilla. Under this mapping, the quasi-Hermitian Hilbert-Schmidt product becomes

$$\text{Tr}(W_1^\dagger W_2) = \langle W_1 | W_2 \rangle_{\eta_+ \otimes \eta_+^{-1}}, \quad (58)$$

with a detailed proof provided in Appendix E. Consequently, the geometric amplitude admits an equivalent pure-state representation

$$\mathcal{G} = \langle W(0) | W(\tau) \rangle. \quad (59)$$

Thus, the Hilbert-Schmidt inner product between initial and final purifications can be interpreted as the Loschmidt amplitude, i.e. the Uhlmann fidelity between the corresponding purified states in the enlarged Hilbert space [63, 66, 67]. The quasi-Hermitian Uhlmann phase $\theta_U^{\eta+} = \arg \mathcal{G}$ is therefore directly encoded in the complex overlap of these two pure states.

To access the complex amplitude \mathcal{G} , one can implement an ancilla-assisted interferometric protocol [68, 69]. By introducing an additional control qubit and performing controlled state preparation for the initial and final purifications, the joint system is prepared in the entangled superposition

$$\frac{1}{\sqrt{2}}(|0\rangle_c \otimes |W(0)\rangle + |1\rangle_c \otimes |W(\tau)\rangle). \quad (60)$$

Measurements of σ_x and σ_y on the control qubit then yield the real and imaginary parts of \mathcal{G} , respectively, enabling direct measurement of the Uhlmann phase.

For the two-level models considered in this work, the experimental implementation requires minimal quantum resources: a single system qubit, one ancilla qubit for purification, and one control qubit for interferometric readout. The relevant unitaries can be decomposed into elementary gates: the state preparation of $|W(0)\rangle$ and $|W(\tau)\rangle$ requires only parameterized single-qubit rotations, while the controlled operations can be realized with standard CNOT gates. These resource requirements are well within the capabilities of current quantum processors, including superconducting platforms such as IBM Quantum devices, where high-fidelity single- and two-qubit gates are routinely available. For instance, the controlled preparation of $|W(\tau)\rangle$ can be implemented by first preparing $|W(0)\rangle$ and then applying a parameterized circuit that implements the unitary $U(\tau)$ conditional on the control qubit.

Since \mathcal{G} is directly accessible within this interferometric framework, finite-temperature geometric phase transitions acquire a clear experimental signature. The transition is characterized by the vanishing of the Loschmidt amplitude, $\mathcal{G} = 0$, which manifests experimentally as the loss of interference contrast in the control qubit. By systematically varying the effective temperature (e.g., by tuning the populations in the density matrix through controlled initialization) and tracking the measured overlap signal, the critical points can be directly identified. This provides a concrete and experimentally viable pathway for probing quasi-Hermitian mixed-state geometric phases and their temperature-driven transitions on quantum information platforms.

VI. CONCLUSION

In this work, we have established a comprehensive theoretical framework for the Uhlmann phase in quasi-Hermitian quantum systems. Recognizing that the standard purification $\rho = WW^\dagger$ is incompatible with non-Hermitian structures, we introduced a generalized amplitude decomposition $\rho = WW^\ddagger$ based on the physical inner product defined by the positive-definite metric operator η_+ . This construction naturally yields a quasi-unitary gauge group $U_{\eta_+}(N)$ and a parallel transport condition that minimizes the η_+ -weighted Hilbert-Schmidt distance. The resulting Uhlmann connection

and its holonomy provide a gauge-invariant characterization of the geometric phase for mixed states in systems with parameter-dependent inner products.

Our analysis reveals that the geometric structure of quasi-Hermitian mixed states is profoundly richer than that of their Hermitian counterparts. The dynamic metric $\eta_+(\lambda)$ actively participates in the parallel transport, introducing an emergent geometric contribution that fundamentally alters the criteria for topological phase transitions. Using exactly solvable two-level models, we demonstrated that the Uhlmann phase can undergo multiple transitions between topologically trivial ($\theta_V^\eta = 0$) and nontrivial ($\theta_V^\eta = \pi$) regimes as temperature varies. The number and location of these transitions are controlled by both the winding number Ω and the quasi-Hermitian parameters. Remarkably, unlike in Hermitian systems where nontrivial topology is typically a low-temperature phenomenon, the quasi-Hermitian framework permits nontrivial phases to persist within specific finite-temperature windows or even emerge exclusively at intermediate temperatures.

Furthermore, we have shown that the quasi-Hermitian Uhlmann phase is experimentally accessible via an ancilla-assisted interferometric protocol, where the geometric amplitude is encoded as a measurable Loschmidt overlap between purified states. The required quantum resources are minimal and well within the capabilities of existing quantum-information platforms, providing a practical pathway for probing finite-temperature geometric phase transitions in non-Hermitian systems.

These findings highlight the intricate interplay between thermal fluctuations, non-Hermiticity, and geometric phases. The theory developed here provides a foundation for investigating finite-temperature topology in a broad class of non-Hermitian systems, including open quantum systems, optical platforms with gain and loss, and correlated materials described by effective non-Hermitian Hamiltonians. Future directions include extending this framework to higher-dimensional parameter spaces and interacting many-body systems, elucidating its connections with quantum geometric tensors and non-Hermitian topological invariants, and systematically exploring the geometric role of parameter-dependent metrics in more general pseudo-Hermitian and genuinely complex-spectral settings. Advancing along these lines promises deeper insight into the structure of non-Hermitian quantum geometry and its interplay with thermodynamic phenomena.

VII. ACKNOWLEDGEMENTS

H. G. was supported by the Innovation Program for Quantum Science and Technology-National Science and Technology Major Project (Grant No. 2021ZD0301904) and the National Natural Science Foundation of China (Grant No. 12447216). X.-Y. H was supported by the National Natural Science Foundation of China (Grant

No. 12405008).

Appendix A: Derivation of the Uhlmann Parallel Transport Condition from Hilbert–Schmidt Distance Minimization

In quasi-Hermitian systems, the density matrix can be written as $\rho = WW^\ddagger$, where the purification (amplitude) W possesses a gauge redundancy $W \sim WU$ with $U \in U_{\eta_+}(N)$ satisfying $U^\ddagger U = UU^\ddagger = \mathbb{I}$. To select the most natural lift among the gauge degrees of freedom, we introduce the physical Hilbert–Schmidt distance on the purification space:

$$D_{\text{HS}}^2(W_1, W_2) := \text{Tr}_{\eta_+} [(W_1 - W_2)^\ddagger (W_1 - W_2)], \quad (\text{A1})$$

where $\text{Tr}_{\eta_+}(X) := \text{Tr}(\eta_+ X)$. Given two neighboring parameter points λ and $\lambda + d\lambda$, we denote $W_1 := W(\lambda)$ and $W_2 := W(\lambda + d\lambda)$. Since the purification at the second point can undergo a gauge transformation, we consider minimizing the function over all $U \in U_{\eta_+}(N)$:

$$\begin{aligned} F(U) &:= D_{\text{HS}}^2(W_1, W_2 U) \\ &= \text{Tr}_{\eta_+} [(W_1 - W_2 U)^\ddagger (W_1 - W_2 U)]. \end{aligned} \quad (\text{A2})$$

Expanding (A2) and using $U^\ddagger U = \mathbb{I}$ yields

$$\begin{aligned} F(U) &= \text{Tr}_{\eta_+}(W_1^\ddagger W_1) + \text{Tr}_{\eta_+}(U^\ddagger W_2^\ddagger W_2 U) \\ &\quad - \text{Tr}_{\eta_+}(W_1^\ddagger W_2 U) - \text{Tr}_{\eta_+}(U^\ddagger W_2^\ddagger W_1) \\ &= \text{Tr}_{\eta_+}(W_1^\ddagger W_1) + \text{Tr}_{\eta_+}(W_2^\ddagger W_2) \\ &\quad - 2 \text{Re} \text{Tr}_{\eta_+}(W_1^\ddagger W_2 U), \end{aligned} \quad (\text{A3})$$

where in the second line we used $\text{Tr}_{\eta_+}(U^\ddagger X U) = \text{Tr}_{\eta_+}(X)$ (since U is η_+ -unitary). Hence minimizing $F(U)$ is equivalent to maximizing

$$G(U) := \text{Re} \text{Tr}_{\eta_+}(W_1^\ddagger W_2 U). \quad (\text{A4})$$

To find the extremum condition, consider an infinitesimal variation of U . Since $U \in U_{\eta_+}(N)$, we can write

$$U \rightarrow U e^{\epsilon K}, \quad K^\ddagger = -K, \quad \epsilon \in \mathbb{R}, \quad |\epsilon| \ll 1, \quad (\text{A5})$$

so that $\delta U = \epsilon U K$ and $\delta U^\ddagger = -\epsilon K U^\ddagger$. Taking the first variation of (A4) gives

$$\delta G = \epsilon \text{Re} \text{Tr}_{\eta_+} \left(W_1^\ddagger W_2 U K \right). \quad (\text{A6})$$

The extremum requires $\delta G = 0$ for all anti-self-adjoint $K^\ddagger = -K$, i.e.,

$$\text{Re} \text{Tr}_{\eta_+}(AK) = 0, \quad A := W_1^\ddagger W_2 U. \quad (\text{A7})$$

Any operator can be decomposed into \ddagger -self-adjoint and \ddagger -anti-self-adjoint parts: $A = A_h + A_a$ with $A_h = \frac{1}{2}(A + A^\ddagger)$, $A_a = \frac{1}{2}(A - A^\ddagger)$. For any $K^\ddagger = -K$, $\text{Tr}_{\eta_+}(A_h K)$ is

purely imaginary while $\text{Tr}_{\eta_+}(A_a K)$ is purely real. Therefore condition (A7) holds for all anti-self-adjoint K if and only if

$$A_a = \frac{1}{2}(A - A^\ddagger) = 0 \iff A = A^\ddagger. \quad (\text{A8})$$

Thus, at the extremal gauge we must have

$$(W_1^\ddagger W_2 U)^\ddagger = W_1^\ddagger W_2 U, \quad (\text{A9})$$

i.e., $W_1^\ddagger W_2 U$ is \ddagger -self-adjoint. Moreover, in the full-rank case, the solution that maximizes (A4) corresponds to the \ddagger -polar decomposition of $W_1^\ddagger W_2 U$, with the optimal choice making this operator positive definite (positive spectrum), often written as

$$W_1^\ddagger W_2 U > 0. \quad (\text{A10})$$

This condition is the discrete version of the Uhlmann parallel condition commonly found in the literature.

Finally, we take the continuum limit. Set $W_2 = W_1 + dW$ with $dW = \dot{W} d\lambda$, and choose the extremal gauge such that $U = \mathbb{I} + \mathcal{O}(d\lambda)$. From the \ddagger -self-adjointness required by (A10), the expression $W^\ddagger(\lambda)W(\lambda + d\lambda) = W^\ddagger W + W^\ddagger dW$ must remain \ddagger -self-adjoint to first order, so its first-order correction must satisfy

$$(W^\ddagger dW)^\ddagger = W^\ddagger dW. \quad (\text{A11})$$

Noting that $(W^\ddagger dW)^\ddagger = dW^\ddagger W$, we obtain

$$W^\ddagger dW = dW^\ddagger W. \quad (\text{A12})$$

Dividing both sides by $d\lambda$ yields

$$W^\ddagger \dot{W} = \dot{W}^\ddagger W, \quad (\text{A13})$$

which is the Uhlmann parallel transport condition for mixed states in quasi-Hermitian systems.

Appendix B: Derivation of the Quasi-Hermitian Uhlmann Connection from the Parallel Evolution Condition

Here we provide a detailed derivation of the quasi-Hermitian Uhlmann connection directly from the quasi-Hermitian parallel evolution condition, demonstrating how the form of the connection is uniquely determined by the parallel transport condition.

Consider a parameter path $\lambda \mapsto \rho(\lambda)$ with the corresponding purification representation

$$\rho(\lambda) = W(\lambda)W^\ddagger(\lambda), \quad (\text{B1})$$

where \ddagger denotes the adjoint operation defined with respect to the quasi-Hermitian physical inner product. The Uhlmann parallel evolution condition for mixed states in quasi-Hermitian systems reads

$$W^\ddagger \dot{W} = \dot{W}^\ddagger W, \quad (\text{B2})$$

with $\dot{(\cdot)} \equiv d/d\lambda$.

In the full-rank case, we employ the gauge decomposition introduced in the main text:

$$W(\lambda) = \sqrt{\rho(\lambda)} U(\lambda), \quad U^\dagger U = \mathbb{I}, \quad (\text{B3})$$

where $U(\lambda)$ takes values in the quasi-unitary group $U_{\eta_+}(N)$. Differentiating W gives

$$\dot{W} = \dot{\sqrt{\rho}} U + \sqrt{\rho} \dot{U}. \quad (\text{B4})$$

Using the property $(AB)^\dagger = B^\dagger A^\dagger$ and the constraint $U^\dagger U = \mathbb{I}$, we compute

$$\begin{aligned} W^\dagger \dot{W} &= U^\dagger \dot{\sqrt{\rho}} (\dot{\sqrt{\rho}} U + \sqrt{\rho} \dot{U}) \\ &= U^\dagger (\dot{\sqrt{\rho}} \dot{\sqrt{\rho}}) U + U^\dagger \rho \dot{U}, \end{aligned} \quad (\text{B5})$$

$$\begin{aligned} \dot{W}^\dagger W &= (\dot{U}^\dagger \sqrt{\rho} + U^\dagger \dot{\sqrt{\rho}}) \sqrt{\rho} U \\ &= \dot{U}^\dagger \rho U + U^\dagger (\dot{\sqrt{\rho}} \sqrt{\rho}) U. \end{aligned} \quad (\text{B6})$$

Substituting these results into the parallel evolution condition and multiplying on the left by U and on the right by U^\dagger , we obtain

$$\sqrt{\rho} \dot{\sqrt{\rho}} + \rho \dot{U} U^\dagger = \dot{\sqrt{\rho}} \sqrt{\rho} + \dot{U}^\dagger U \rho. \quad (\text{B7})$$

Differentiating the identity $U^\dagger U = \mathbb{I}$ yields

$$\dot{U}^\dagger U = -U^\dagger \dot{U}. \quad (\text{B8})$$

Introducing the definition of the quasi-Hermitian Uhlmann connection $\mathcal{A}_U^{\eta_+} := -dUU^\dagger$, and substituting into (B7), we obtain

$$\sqrt{\rho} d\sqrt{\rho} - \rho \mathcal{A}_U^{\eta_+} = d\sqrt{\rho} \sqrt{\rho} + \mathcal{A}_U^{\eta_+} \rho. \quad (\text{B9})$$

Rearranging gives the Sylvester-type equation satisfied by $\mathcal{A}_U^{\eta_+}$:

$$\rho \mathcal{A}_U^{\eta_+} + \mathcal{A}_U^{\eta_+} \rho = -[d\sqrt{\rho}, \sqrt{\rho}]. \quad (\text{B10})$$

Thus, the quasi-Hermitian Uhlmann connection is uniquely determined by the parallel evolution condition, its form depending solely on the variation of the mixed-state density matrix along the parameter path. The geometric phase for quasi-Hermitian mixed states discussed in the main text is precisely the holonomy induced by this connection in parameter space.

Appendix C: Comparison of Uhlmann Connection and Phase under Similarity Transformations: Quasi-Hermitian vs. Hermitian Formulations

We have constructed parallel transport, the Uhlmann connection, and the induced geometric phase for mixed states within the quasi-Hermitian framework. This construction is based on the physical inner product defined

by the positive-definite metric $\eta_+(\lambda)$ and takes the quasi-Hermitian parallel transport condition as the starting point for the geometric structure of mixed states.

In this framework, the introduction of a positive-definite metric implies that at each fixed parameter point, the quasi-Hermitian Hamiltonian can be mapped to a Hermitian operator under the Dirac inner product via an appropriate similarity transformation [70]. Thus, the quasi-Hermitian formulation is not independent of Hermitian quantum mechanics but rather constitutes an equivalent description reparameterized by the inner product structure. This naturally raises the question: under the correspondence established by the similarity transformation, does the Uhlmann connection (a local geometric object) defined in the quasi-Hermitian formulation and the induced Uhlmann phase (the global consequence of the holonomy) coincide with those in the corresponding Hermitian formulation? If not, how should the discrepancy be interpreted through the geometry of the purification space?

To concretely compare the geometric structures in the two formulations, we introduce a similarity transformation operator $S(\lambda)$ such that the quasi-Hermitian Hamiltonian $H(\lambda)$ and the Hermitian Hamiltonian $h(\lambda)$ satisfy

$$h(\lambda) = S(\lambda) H(\lambda) S^{-1}(\lambda), \quad h^\dagger(\lambda) = h(\lambda). \quad (\text{C1})$$

Under the quasi-Hermitian conventions adopted in this paper, the metric operator can be taken as

$$\eta_+(\lambda) = S^\dagger(\lambda) S(\lambda), \quad (\text{C2})$$

so that under the similarity transformation S , an operator A that is self-adjoint in the quasi-Hermitian sense ($A^\dagger = A$) is mapped to a Hermitian operator in the Dirac sense ($(SAS^{-1})^\dagger = SAS^{-1}$).

From the perspective of Lie-group theory, it is worth noting that the quasi-unitary group $U_{\eta_+(\lambda)}(N)$ defined by $U^\dagger U = \mathbb{I}$ is isomorphic to the standard unitary group $U(N)$ via the similarity transformation $S(\lambda)$. Specifically, the conjugation map $\tilde{U} = SUS^{-1}$ establishes a one-to-one correspondence between quasi-unitary and unitary operators. Hence, at each fixed parameter point, the two groups are identical as Lie groups. The distinction between the quasi-Hermitian and Hermitian formulations therefore does not arise from their algebraic structure, but rather from the way this symmetry group is fibered over the parameter space when $S(\lambda)$ (equivalently $\eta_+(\lambda)$) depends on the external parameters. This parameter-dependent fibration is precisely what gives rise to the additional geometric features explored in this work.

Under this similarity transformation, the biorthogonal eigenstates $\{|\Psi_n\rangle, \langle\Phi_n|\}$ of the quasi-Hermitian Hamiltonian are mapped to orthonormal eigenstates in the Hermitian formulation:

$$|n(\lambda)\rangle := S(\lambda) |\Psi_n(\lambda)\rangle, \quad \langle n(\lambda)| := \langle\Phi_n(\lambda)| S^{-1}(\lambda), \quad (\text{C3})$$

satisfying $h(\lambda)|n(\lambda)\rangle = E_n(\lambda)|n(\lambda)\rangle$ and $\langle n(\lambda)|m(\lambda)\rangle = \delta_{nm}$. Correspondingly, the density matrix in the Hermitian formulation is defined as

$$\rho_h(\lambda) := S(\lambda)\rho(\lambda)S^{-1}(\lambda), \quad (\text{C4})$$

whose spectral decomposition is naturally given in the orthonormal basis $\{|n(\lambda)\rangle\}$. In this Hermitian formulation, the geometric structure of mixed states can be constructed following the standard Uhlmann theory: the Uhlmann connection \mathcal{A}_U^h corresponding to the path $\rho_h(\lambda)$ is uniquely determined by $\rho_h(\lambda)$ and takes the explicit form

$$\mathcal{A}_U^h = - \sum_{m,n} |m\rangle \frac{\langle m|[d\sqrt{\rho_h}, \sqrt{\rho_h}]|n\rangle}{p_m + p_n} \langle n|, \quad (\text{C5})$$

where $\{|n\rangle\}$ are the orthonormal eigenstates of ρ_h and $p_n > 0$ are the corresponding eigenvalues.

Comparing this with the Uhlmann connection obtained in the quasi-Hermitian formulation, Eq. (26), we see that the two expressions are structurally identical but are built on different inner product structures: the former acts on the density matrix path $\rho_h(\lambda)$ under the Dirac inner product, while the latter corresponds to the path $\rho(\lambda)$ under the physical inner product defined by the metric operator $\eta_+(\lambda)$.

If the similarity transformation S is constant in parameter space (equivalently, if the metric operator η_+ does not vary with parameters), then ρ_h and ρ differ only by a fixed basis transformation. In this case, the Uhlmann connections in the two formulations satisfy the simple covariant relation

$$\mathcal{A}_U^{\eta_+} = S^{-1}\mathcal{A}_U^h S, \quad (\text{C6})$$

and consequently the Uhlmann phases induced along a closed parameter path are identical after taking the trace.

When the similarity transformation $S(\lambda)$ is parameter-dependent, the correspondence between the quasi-Hermitian and Hermitian formulations changes fundamentally. In this case, $S(\lambda)$ is no longer merely a passive reparameterization; through the metric operator $\eta_+(\lambda)$, it introduces a parameter-dependent physical inner product structure. In the quasi-Hermitian formulation, the criterion for "parallel transport" is defined relative to a physical inner product that varies with parameters; in contrast, parallel transport in the Hermitian formulation is always based on the fixed Dirac inner product. This difference implies that the "horizontal" lifts of the path selected in the two formulations are generally not the same. Consequently, the similarity transformation induces an additional connection structure in the purification space, controlled by $dS S^{-1}$ (equivalently $d\eta_+$), such that the Uhlmann connections in the two formulations no longer satisfy a simple covariant relation.

In the quasi-Hermitian formulation, the Uhlmann connection $\mathcal{A}_U^{\eta_+}$ has been obtained in Eq. (26). In the Hermitian representation, the corresponding Uhlmann connection \mathcal{A}_U^h associated with the density-matrix path $\rho_h(\lambda)$

is given by the standard expression Eq. (C5). Using the similarity transformation relations $\rho_h = S\rho S^{-1}$ and $\sqrt{\rho_h} = S\sqrt{\rho}S^{-1}$, and applying the similarity transformation to Eq. (26), we obtain

$$S\mathcal{A}_U^{\eta_+} S^{-1} = - \sum_{m,n} |m\rangle \frac{\langle m|S[d\sqrt{\rho}, \sqrt{\rho}]S^{-1}|n\rangle}{p_m + p_n} \langle n|. \quad (\text{C7})$$

The key difference arises from the differential of the square root operator. From $\sqrt{\rho_h} = S\sqrt{\rho}S^{-1}$, its differential is

$$d\sqrt{\rho_h} = (dS)\sqrt{\rho}S^{-1} + S(d\sqrt{\rho})S^{-1} + S\sqrt{\rho}d(S^{-1}), \quad (\text{C8})$$

Introducing $K = dS S^{-1}$, the differential further becomes

$$d\sqrt{\rho_h} = K\sqrt{\rho_h} + S(d\sqrt{\rho})S^{-1} - \sqrt{\rho_h}K. \quad (\text{C9})$$

From this we compute the commutator

$$[d\sqrt{\rho_h}, \sqrt{\rho_h}] = S[d\sqrt{\rho}, \sqrt{\rho}]S^{-1} + \Delta_S, \quad (\text{C10})$$

where

$$\Delta_S = K\rho_h + \rho_h K - 2\sqrt{\rho_h} K \sqrt{\rho_h}. \quad (\text{C11})$$

Substituting Eq. (C10) into the Hermitian Uhlmann connection (C5) and comparing with Eq. (C7) yields

$$\mathcal{A}_U^h = S\mathcal{A}_U^{\eta_+} S^{-1} - \mathcal{A}_S, \quad (\text{C12})$$

where the additional connection term is

$$\mathcal{A}_S = \sum_{m,n} |m\rangle \frac{\langle m|\Delta_S|n\rangle}{p_m + p_n} \langle n|. \quad (\text{C13})$$

In the eigenbasis of ρ_h , we have $\rho_h|n\rangle = p_n|n\rangle$ and $\sqrt{\rho_h}|n\rangle = \sqrt{p_n}|n\rangle$, so that

$$\langle m|\Delta_S|n\rangle = (p_m + p_n - 2\sqrt{p_m p_n})\langle m|K|n\rangle. \quad (\text{C14})$$

Inserting this into Eq. (C13) gives

$$\mathcal{A}_S = \sum_{m,n} \frac{(\sqrt{p_m} - \sqrt{p_n})^2}{p_m + p_n} |m\rangle \langle m|dS S^{-1}|n\rangle \langle n|. \quad (\text{C15})$$

This term does not originate from the density matrix path itself but reflects the variation of the physical inner product structure along the parameter space, projected onto the relevant Lie algebra directions via the Uhlmann parallel transport condition. When $dS = 0$ (equivalently $d\eta_+ = 0$), this additional term vanishes, restoring the strict equivalence between the quasi-Hermitian and Hermitian formulations at the level of the Uhlmann connection and phase.

It is important to emphasize that the Uhlmann connection is a local geometric object defined on the parameter

space, while the Uhlmann phase is the global quantity induced by the holonomy of this connection along a closed parameter loop. For a closed loop \mathcal{C} in parameter space, the Uhlmann phase in the quasi-Hermitian formulation is defined by the holonomy of the connection $\mathcal{A}_U^{\eta+}$, given by Eq. (28), and remains invariant under quasi-unitary gauge transformations.

In the Hermitian formulation, the corresponding Uhlmann phase is determined by the holonomy of the connection \mathcal{A}_U^h . From Eq. (C15), we see that the difference between the connections in the two formulations is entirely controlled by the additional term \mathcal{A}_S . Since the Uhlmann phase is a global quantity obtained by integrating around a closed loop, this local difference manifests as an extra global contribution after the loop integral. In general, we have

$$\theta_U^h = \theta_U^{\eta+} - \oint_{\mathcal{C}} \Gamma_S, \quad (\text{C16})$$

where Γ_S denotes the contribution induced by \mathcal{A}_S along the loop \mathcal{C} , the specific form of which depends on the chosen horizontal structure and gauge conventions. When this loop contribution vanishes, the Uhlmann phases in the two formulations coincide; otherwise, the parameter-dependent physical inner product leads to a discernible difference between the quasi-Hermitian and Hermitian Uhlmann phases.

When the metric reduces to the identity operator (in which case one can take S to be unitary and $dS = 0$), the additional term \mathcal{A}_S disappears, and the above structure continuously reduces to the standard Uhlmann theory in Hermitian quantum mechanics.

In summary, this appendix demonstrates that while the similarity transformation ensures consistency between the quasi-Hermitian and Hermitian formulations at the level of spectral and probabilistic structures, at the level of the mixed-state geometric structure, a parameter-dependent similarity transformation introduces an additional connection term that modifies the parallel transport rule, leading to nontrivial deviations in the Uhlmann connection and consequently in the Uhlmann phase.

Appendix D: Analytic Derivation of the Quasi-Hermitian Uhlmann Holonomy on an Equatorial Loop

Here we provide the analytic derivation of the Uhlmann holonomy for an equatorial closed loop given in Eq. (52) of the main text.

The Uhlmann holonomy along an equatorial path $\phi \in [0, 2\pi\Omega]$ is defined as

$$U(2\pi\Omega) = \mathcal{P} \exp \left(\int_0^{2\pi\Omega} A_\phi(\phi) d\phi \right), \quad (\text{D1})$$

where $A_U^{\eta+} = A_\phi(\phi) d\phi$ with

$$A_\phi(\phi) = \kappa \left[\frac{a^2}{2\Delta^2} i \sigma_z - \frac{ab}{2\Delta^2} e^{-i\phi\sigma_z/2} \sigma_x e^{i\phi\sigma_z/2} \right] d\phi. \quad (\text{D2})$$

The path-ordered exponential is equivalent to solving the initial value problem

$$\frac{d}{d\phi} U(\phi) = A_\phi(\phi) U(\phi), \quad U(0) = \mathbb{I}. \quad (\text{D3})$$

Introduce the rotation operator about the z -axis:

$$R(\phi) = \exp(-\phi\sigma_z/2), \quad (\text{D4})$$

and perform a change of variables to a rotating frame:

$$U(\phi) = R(\phi) \tilde{U}(\phi). \quad (\text{D5})$$

Substituting Eq. (D5) into the differential equation (D3) and multiplying on the left by $R^{-1}(\phi)$ yields

$$\frac{d}{d\phi} \tilde{U}(\phi) = \tilde{A}_\phi \tilde{U}(\phi), \quad \tilde{A}_\phi := R^{-1} A_\phi R - R^{-1} \frac{dR}{d\phi}. \quad (\text{D6})$$

Using $R^{-1}\sigma_z R = \sigma_z$, we obtain

$$R^{-1}(\phi) A_\phi(\phi) R(\phi) = \kappa \left[\frac{a^2}{2\Delta^2} i \sigma_z - \frac{ab}{2\Delta^2} \sigma_x \right], \quad (\text{D7})$$

and from Eq. (D4) we directly compute

$$\frac{dR}{d\phi} = -\frac{i}{2} \sigma_z R(\phi) \Rightarrow R^{-1} \frac{dR}{d\phi} = -\frac{i}{2} \sigma_z. \quad (\text{D8})$$

Substituting into Eq. (D6) gives a ϕ -independent constant generator

$$\tilde{A}_\phi = i \left(\frac{a^2}{2\Delta^2} \kappa + \frac{1}{2} \right) \sigma_z - \frac{ab}{2\Delta^2} \kappa \sigma_x. \quad (\text{D9})$$

Therefore,

$$\tilde{U}(\phi) = \exp(\phi \tilde{A}_\phi), \quad (\text{D10})$$

and consequently

$$U(2\pi\Omega) = R(2\pi\Omega) \exp(2\pi\Omega \tilde{A}_\phi). \quad (\text{D11})$$

Noting that

$$R(2\pi\Omega) = \exp(-i\pi\Omega\sigma_z) = (-1)^{\Omega\mathbb{I}}, \quad (\text{D12})$$

we finally obtain the closed-form result

$$U(2\pi\Omega) = (-1)^{\Omega\mathbb{I}} e^{2\pi\Omega \left[i \left(\frac{a^2}{2\Delta^2} \kappa + \frac{1}{2} \right) \sigma_z - \frac{ab}{2\Delta^2} \kappa \sigma_x \right]}. \quad (\text{D13})$$

Appendix E: Equivalence between the quasi-Hermitian Hilbert–Schmidt product and the Loschmidt amplitude

Here we prove that, under the vectorization (purification) map, the quasi-Hermitian Hilbert–Schmidt inner product between two amplitudes is equivalent to the overlap (Loschmidt amplitude/fidelity) between the corresponding purified states in the enlarged space:

$$\mathrm{Tr}\left(W_1^\dagger W_2\right) = \langle W_1|W_2\rangle_{\eta_+ \otimes \eta_+^{-1}}. \quad (\text{E1})$$

We start from the spectral-form purifications

$$W = \sum_n \sqrt{p_n} |\psi_n\rangle \langle \phi_n| \mathcal{U}, \quad (\text{E2})$$

and define the corresponding purified states

$$|W\rangle = \sum_n \sqrt{p_n} |\psi_n\rangle_S \otimes \mathcal{U}^T |\phi_n\rangle_A. \quad (\text{E3})$$

The metric-weighted inner product in the enlarged space is

$$\langle W_1|W_2\rangle_{\eta_+ \otimes \eta_+^{-1}} := \langle W_1|(\eta_+ \otimes \eta_+^{-1})|W_2\rangle. \quad (\text{E4})$$

Substituting Eq. (E3) gives

$$\langle W_1|W_2\rangle_{\eta_+ \otimes \eta_+^{-1}}$$

$$\begin{aligned} &= \sum_{mn} \sqrt{p_n} \sqrt{p_m} \langle \psi_n|\eta_+|\psi_m\rangle \langle \phi_m|\mathcal{U}_2\eta_+^{-1}\mathcal{U}_1^\dagger|\phi_n\rangle \\ &= \sum_{mn} p_n \delta_{mn} \langle \phi_m|\mathcal{U}_2\eta_+^{-1}\mathcal{U}_1^\dagger\eta_+|\psi_n\rangle \\ &= \sum_n p_n \langle \phi_n|\mathcal{U}_2\mathcal{U}_1^\dagger|\psi_n\rangle \\ &= \mathrm{Tr}_{\eta_+}(\rho\mathcal{U}_2\mathcal{U}_1^\dagger). \end{aligned} \quad (\text{E5})$$

It is important to note that, in the above derivation, the factor $\mathcal{U}^T|\phi_n\rangle$ in the purified state is to be treated as a bra.

On the other hand, a direct evaluation of the quasi-Hermitian Hilbert–Schmidt product yields

$$\begin{aligned} &\mathrm{Tr}_{\eta_+}(W_1^\dagger W_2) \\ &= \mathrm{Tr}_{\eta_+}\left(\sum_n \mathcal{U}_1^\dagger \sqrt{p_n} \eta^{-1} |\phi_n\rangle \langle \psi_n| \eta \sum_m \sqrt{p_m} |\psi_m\rangle \langle \phi_m| \mathcal{U}_2\right) \\ &= \mathrm{Tr}_{\eta_+}\left(\sum_n \mathcal{U}_1^\dagger \sqrt{p_n} |\psi_n\rangle \langle \phi_n| \sum_m \sqrt{p_m} |\psi_m\rangle \langle \phi_m| \mathcal{U}_2\right) \\ &= \mathrm{Tr}_{\eta_+}\left(\sum_{m,n} \mathcal{U}_1^\dagger \sqrt{p_n} \sqrt{p_m} |\psi_n\rangle \delta_{mn} \langle \phi_m| \mathcal{U}_2\right) \\ &= \mathrm{Tr}_{\eta_+}\left(\sum_n p_n |\psi_n\rangle \langle \phi_n| \mathcal{U}_2 \mathcal{U}_1^\dagger\right) \\ &= \mathrm{Tr}_{\eta_+}(\rho\mathcal{U}_2\mathcal{U}_1^\dagger). \end{aligned} \quad (\text{E6})$$

Therefore, the geometric amplitude can be viewed as the Loschmidt (fidelity) amplitude between the initial and final purifications.

-
- [1] S. Pancharatnam, Generalized theory of interference, and its applications, Proceedings of the Indian Academy of Sciences - Section A **44**, 247 (1956).
- [2] M. V. Berry, Quantal phase factors accompanying adiabatic changes, Proceedings of the Royal Society of London A **392**, 45 (1984).
- [3] E. Sjöqvist, A. K. Pati, A. Ekert, J. S. Anandan, M. Ericsson, D. K. L. Oi, and V. Vedral, Geometric phases for mixed states in interferometry, Phys. Rev. Lett. **85**, 2845 (2000).
- [4] M. Ericsson, E. Sjöqvist, J. Brännlund, D. K. L. Oi, and A. K. Pati, Generalization of the geometric phase to completely positive maps, Phys. Rev. A **67**, 020101 (2003).
- [5] A. Carollo, I. Fuentes-Guridi, M. F. m. c. Santos, and V. Vedral, Geometric phase in open systems, Phys. Rev. Lett. **90**, 160402 (2003).
- [6] J. G. P. d. Faria, A. F. R. d. T. Piza, and M. C. Nemes, Phases of quantum states in completely positive non-unitary evolution, Europhysics Letters (EPL) **62**, 782–788 (2003).
- [7] J. Du, P. Zou, M. Shi, L. C. Kwek, J.-W. Pan, C. H. Oh, A. Ekert, D. K. L. Oi, and M. Ericsson, Observation of geometric phases for mixed states using nmr interferometry, Phys. Rev. Lett. **91**, 100403 (2003).
- [8] J. Klepp, S. Sponar, S. Filipp, M. Lettner, G. Badurek, and Y. Hasegawa, Observation of nonadditive mixed-state phases with polarized neutrons, Phys. Rev. Lett. **101**, 150404 (2008).
- [9] M. Ericsson, D. Achilles, J. T. Barreiro, D. Branning, N. A. Peters, and P. G. Kwiat, Measurement of geometric phase for mixed states using single photon interferometry, Phys. Rev. Lett. **94**, 050401 (2005).
- [10] A. Uhlmann, Parallel transport and “quantum holonomy” along density operators, Rep. Math. Phys. **24**, 229 (1986).
- [11] A. Uhlmann, On berry phases along mixtures of states, Ann. Phys. (Berlin) **501**, 63 (1989).
- [12] A. Uhlmann, A gauge field governing parallel transport along mixed states, Lett. Math. Phys. **21**, 229 (1991).
- [13] A. Uhlmann, Geometric phases and related structures, Reports on Mathematical Physics **36**, 461 (1995).
- [14] O. Viyuela, A. Rivas, and M. A. Martin-Delgado, Uhlmann phase as a topological measure for one-dimensional fermion systems, Phys. Rev. Lett. **112**, 130401 (2014).
- [15] O. Viyuela, A. Rivas, and M. A. Martin-Delgado, Two-dimensional density-matrix topological fermionic phases: Topological uhlmann numbers, Phys. Rev. Lett. **113**, 076408 (2014).
- [16] H. Guo, X.-Y. Hou, Y. He, and C. C. Chien, Dynamic process and uhlmann process: Incompatibility and dynamic phase of mixed quantum states, Phys. Rev. B **101**,

- 104310 (2020).
- [17] X.-Y. Hou, Q.-C. Gao, H. Guo, Y. He, T. Liu, and C. C. Chien, Ubiquity of zeros of the loschmidt amplitude for mixed states in different physical processes and its implication, *Phys. Rev. B* **102**, 104305 (2020).
- [18] D. Morachis Galindo, F. Rojas, and J. A. Maytorena, Topological uhlmann phase transitions for a spin- j particle in a magnetic field, *Phys. Rev. A* **103**, 042221 (2021).
- [19] Y. Zhang, A. Pi, Y. He, and C.-C. Chien, Comparison of finite-temperature topological indicators based on uhlmann connection, *Phys. Rev. B* **104**, 165417 (2021).
- [20] X.-Y. Hou, H. Guo, and C.-C. Chien, Finite-temperature topological phase transitions of spin- j systems in uhlmann processes: General formalism and experimental protocols, *Phys. Rev. A* **104**, 023303 (2021).
- [21] X.-Y. Hou, X. Wang, Z. Zhou, H. Guo, and C.-C. Chien, Geometric phases of mixed quantum states: A comparative study of interferometric and uhlmann phases, *Phys. Rev. B* **107**, 165415 (2023).
- [22] O. Viyuela, A. Rivas, and M. A. Martin-Delgado, Uhlmann phase as a topological measure for one-dimensional fermion systems, *Phys. Rev. Lett.* **112**, 130401 (2014).
- [23] O. Viyuela, A. Rivas, and M. A. Martin-Delgado, Two-dimensional density-matrix topological fermionic phases: Topological uhlmann numbers, *Phys. Rev. Lett.* **113**, 076408 (2014).
- [24] Z. Huang and D. P. Arovas, Topological indices for open and thermal systems via uhlmann's phase, *Phys. Rev. Lett.* **113**, 076407 (2014).
- [25] A. D. Kiselev and V. V. Kesaev, Interferometric and uhlmann phases of mixed polarization states, *Phys. Rev. A* **98**, 033816 (2018).
- [26] J. Villavicencio, E. Cota, F. Rojas, J. A. Maytorena, and D. M. Galindo, Uhlmann phase in composite systems with entanglement, *Phys. Rev. A* **104**, 042204 (2021).
- [27] D. Morachis Galindo, F. Rojas, and J. A. Maytorena, Topological uhlmann phase transitions for a spin- j particle in a magnetic field, *Phys. Rev. A* **103**, 042221 (2021).
- [28] J.-C. Tang, X.-Y. Hou, Z. Zhou, H. Guo, and C.-C. Chien, Uhlmann quench and geometric dynamic quantum phase transition of mixed states, *Phys. Rev. B* **110**, 134319 (2024).
- [29] X. Wang, J.-C. Tang, X.-Y. Hou, H. Guo, and C.-C. Chien, Mixed-state geometric phases of coherent and squeezed spin states, *Phys. Rev. B* **111**, 235450 (2025).
- [30] X. Wang, X.-Y. Hou, Y. He, and H. Guo, Thermal uhlmann-chern number: Bridging pure and mixed states, *Phys. Rev. B* **112**, 214112 (2025).
- [31] N. Hatano and D. R. Nelson, Localization transitions in non-hermitian quantum mechanics, *Phys. Rev. Lett.* **77**, 570 (1996).
- [32] Z. Gong, M. Bello, D. Malz, and F. K. Kunst, Anomalous behaviors of quantum emitters in non-hermitian baths, *Phys. Rev. Lett.* **129**, 223601 (2022).
- [33] F. Roccati, S. Lorenzo, G. Calajò, G. M. Palma, A. Carollo, and F. Ciccarello, Exotic interactions mediated by a non-hermitian photonic bath, *Optica* **9**, 565 (2022).
- [34] Z. Gong, Y. Ashida, K. Kawabata, K. Takasan, S. Higashikawa, and M. Ueda, Topological phases of non-hermitian systems, *Phys. Rev. X* **8**, 031079 (2018).
- [35] F. K. Kunst, E. Edvardsson, J. C. Budich, and E. J. Bergholtz, Biorthogonal bulk-boundary correspondence in non-hermitian systems, *Phys. Rev. Lett.* **121**, 026808 (2018).
- [36] F. Roccati, M. Bello, Z. Gong, M. Ueda, F. Ciccarello, A. Chenu, and A. Carollo, Hermitian and non-hermitian topology from photon-mediated interactions, *Nat. Commun.* **15**, 2400 (2024).
- [37] S. Yao and Z. Wang, Edge states and topological invariants of non-hermitian systems, *Phys. Rev. Lett.* **121**, 086803 (2018).
- [38] J. Li, A. K. Harter, J. Liu, L. de Melo, Y. N. Joglekar, and L. Luo, Observation of parity-time symmetry breaking transitions in a dissipative floquet system of ultracold atoms, *Nature Communications* **10**, 855 (2019).
- [39] L. Xiao, K. Wang, X. Zhan, Z. Bian, K. Kawabata, M. Ueda, W. Yi, and P. Xue, Observation of critical phenomena in parity-time-symmetric quantum dynamics, *Phys. Rev. Lett.* **123**, 230401 (2019).
- [40] Y. Wu, W. Liu, J. Geng, X. Song, X. Ye, C.-K. Duan, X. Rong, and J. Du, Observation of parity-time symmetry breaking in a single-spin system, *Science* **364**, 878 (2019).
- [41] L. Ding, K. Shi, Q. Zhang, D. Shen, X. Zhang, and W. Zhang, Experimental determination of \mathcal{PT} -symmetric exceptional points in a single trapped ion, *Phys. Rev. Lett.* **126**, 083604 (2021).
- [42] L. Xiao, T. Deng, K. Wang, W. Yi, and P. Xue, Non-hermitian bulk-boundary correspondence in quantum dynamics, *Nature Physics* **16**, 761 (2020).
- [43] K. Zhang, Z. Yang, and C. Fang, Correspondence between winding numbers and skin modes in non-hermitian systems, *Phys. Rev. Lett.* **125**, 126402 (2020).
- [44] J. Gong and Q.-h. Wang, Time-dependent \mathcal{PT} -symmetric quantum mechanics, *J. Phys. A: Math. Theor.* **46**, 485302 (2013).
- [45] D.-J. Zhang, Q.-h. Wang, and J. Gong, Quantum geometric tensor in \mathcal{PT} -symmetric quantum mechanics, *Phys. Rev. A* **99**, 042104 (2019).
- [46] W. Pauli, On dirac's new method of field quantization, *Rev. Mod. Phys.* **15**, 175 (1943).
- [47] C. M. Bender and S. Boettcher, Real spectra in non-hermitian hamiltonians having pt symmetry, *Phys. Rev. Lett.* **80**, 5243 (1998).
- [48] A. Mostafazadeh, Pseudo-hermiticity versus pt symmetry: The necessary condition for the reality of the spectrum of a non-hermitian hamiltonian, *J. Math. Phys.* **43**, 205 (2002).
- [49] A. Mostafazadeh, Pseudo-hermiticity versus pt symmetry ii: A complete characterization of non-hermitian hamiltonians with a real spectrum, *J. Math. Phys.* **43**, 2814 (2002).
- [50] A. Mostafazadeh, Pseudo-hermiticity versus pt symmetry iii: Equivalence of pseudo-hermiticity and the presence of antilinear symmetries, *J. Math. Phys.* **43**, 3944 (2002).
- [51] G. L. Giorgi, Spontaneous \mathcal{PT} symmetry breaking and quantum phase transitions in dimerized spin chains, *Phys. Rev. B* **82**, 052404 (2010).
- [52] C. Hang, G. Huang, and V. V. Konotop, \mathcal{PT} symmetry with a system of three-level atoms, *Phys. Rev. Lett.* **110**, 083604 (2013).
- [53] C. Korff and R. Weston, Pt symmetry on the lattice: the quantum group invariant xxz spin chain, *J. Phys. A: Math. Theor.* **40**, 8845 (2007).
- [54] C. Korff, Pt symmetry of the non-hermitian xx spin-chain: non-local bulk interaction from complex boundary

- fields, *J. Phys. A: Math. Theor.* **41**, 295206 (2008).
- [55] V. V. Konotop, J. Yang, and D. A. Zezyulin, Nonlinear waves in \mathcal{PT} -symmetric systems, *Rev. Mod. Phys.* **88**, 035002 (2016).
- [56] C. M. Bender, S. Boettcher, and P. N. Meisinger, \mathcal{PT} -symmetric quantum mechanics, *Journal of Mathematical Physics* **40**, 2201–2229 (1999).
- [57] J. Cham, Top 10 physics discoveries of the last 10 years, *Nature Physics* **11**, 799–799 (2015).
- [58] L. Feng, R. El-Ganainy, and L. Ge, Non-hermitian photonics based on parity–time symmetry, *Nature Photonics* **11**, 752–762 (2017).
- [59] A. MOSTAFAZADEH, Pseudo-hermitian representation of quantum mechanics, *International Journal of Geometric Methods in Modern Physics* **07**, 1191 (2010).
- [60] A. Das, Pseudo-hermitian quantum mechanics, *Journal of Physics: Conference Series* **287**, 012002 (2011).
- [61] D. Chruściński and A. Jamiolkowski, *Geometric Phases in Classical and Quantum Mechanics*, *Progress in Mathematical Physics*, Vol. 36 (Birkhäuser Boston, MA, 2004).
- [62] H. Guo, X.-Y. Hou, Y. He, and C.-C. Chien, Dynamic process and uhlmann process: Incompatibility and dynamic phase of mixed quantum states, *Phys. Rev. B* **101**, 104310 (2020).
- [63] X.-Y. Hou, Q.-C. Gao, H. Guo, Y. He, T. Liu, and C.-C. Chien, Ubiquity of zeros of the loschmidt amplitude for mixed states in different physical processes and its implication, *Phys. Rev. B* **102**, 104305 (2020).
- [64] Q.-h. Wang, S.-z. Chia, and J.-h. Zhang, symmetry as a generalization of hermiticity, *Journal of Physics A: Mathematical and Theoretical* **43**, 295301 (2010).
- [65] A. Bohm, A. Mostafazadeh, H. Koizumi, Q. Niu, and J. Zwanziger, *The Geometric Phase in Quantum Systems: Foundations, Mathematical Concepts, and Applications in Molecular and Condensed Matter Physics* (Springer, Berlin, Heidelberg, 2003).
- [66] M. Heyl, Dynamical quantum phase transitions: a review, *Reports on Progress in Physics* **81**, 054001 (2018).
- [67] D. Mondal and T. Nag, Finite-temperature dynamical quantum phase transition in a non-hermitian system, *Phys. Rev. B* **107**, 184311 (2023).
- [68] O. Viyuela, A. Rivas, S. Gasparinetti, A. Wallraff, S. Filipp, and M. A. Martin-Delgado, Observation of topological uhlmann phases with superconducting qubits, *npj Quantum Information* **4**, 10 (2018).
- [69] C. Mastandrea, C. Iancu, H. Guo, and C.-C. Chien, Intermediate-temperature topological uhlmann phase on ibm quantum computers, *Quantum Science and Technology* **11**, 015033 (2025).
- [70] A. Mostafazadeh, Exact pt-symmetry is equivalent to hermiticity, **36**, 7081 (2003).